Hybrid optical method for characterizing a heliostat field in a concentrated solar power plant

Cite as: AIP Conference Proceedings **2303**, 100002 (2020); https://doi.org/10.1063/5.0029270
Published Online: 11 December 2020

Pierre-Henri Defieux, Cyril Caliot, and François Hénault

Hybrid Optical Method for Characterizing a Heliostat Field in a Concentrated Solar Power Plant

Pierre-Henri Defieux[1, a)], Cyril Caliot[1], François Hénault[2]

[1]*Processes, Materials and Solar Energy laboratory, PROMES CNRS, 7 Rue du Four Solaire, 66120 Font-Romeu-Odeillo-Via, France*
[2]*Institut de Planétologie et d'Astrophysique de Grenoble, IPAG CNRS, Université Grenoble Alpes F-38041 Grenoble, France.*

[a)]Pierre-Henri Defieux : pierre-henri.defieux@promes.cnrs.fr

Abstract. This paper describes the backward-gazing method with four cameras optimized by using different process of data treatments. The method could be useful for the heliostats characterization in a Solar Tower Power Plant (STPP), to detect heliostat pointing errors, mirrors canting and waviness without disturbing the daily electricity production process. The method is based on the use of four cameras near the receiver, all pointing to the heliostat to be characterized, and a fifth one taking images of the Sun. The theoretical principle is explained and different kind of data treatment process are tested and compared by using heliostat images from numerical simulations. Each process model is explained and the software used for simulations is described. The achieved accuracy of the best results is estimated to less than 0.05 mrad RMS in term of surface slopes.

INTRODUCTION

In the context of energetic transition, the development of renewable energies like Solar Tower Power Plant (STPP) is among the most important challenges. The operation principle is to heat and store a fluid in a thermal storage by using several hundreds of focusing heliostats which concentrate solar radiation on a receiver at the top of a tower. The homogeneity and the concentration of the focal spot on the receiver directly affect the conversion efficiency. Thus, the aiming strategy of the heliostat and their optical efficiency are crucial for the development of STPP. Techniques for the alignment and metrology of solar concentrating optics were reviewed in [1]. The backward-gazing method is a new technique patented in 2015 [2] [Fig. 1]. This method was firstly described in 1989 by F. Hénault and C. Royère [3]. Coquand et al. [4] provides the description of the method which is interesting for heliostat characterization, because it could detect simultaneously waviness, mirror canting and heliostat pointing error [4]. This paper describes new image processing techniques and their numerical comparison and validation. The current methods of metrology, like the deflectometry, allow to measure the shape of a heliostat with a precision of 0.2 mrad [4]. The backward-gazing method must have the same accuracy at least, thus we need to test it with simulated data and quantify the effects of noise measurement on the results. The objective is to reach a precision equal to 0.1 mrad with a real measurement, therefore the results from simulated data, which are not contaminated by the measurement noise of cameras, has to be more accurate. The simulation software that used in this study allows to choose the incorporation either of an analytical or of a noisy Sun profile to the simulated data. The comparison between the results with analytical or noisy Sun profile is a first approach to assess the effects of noise on the results.

SolarPACES 2019
AIP Conf. Proc. 2303, 100002-1–100002-11; https://doi.org/10.1063/5.0029270
Published by AIP Publishing. 978-0-7354-4037-1/$30.00

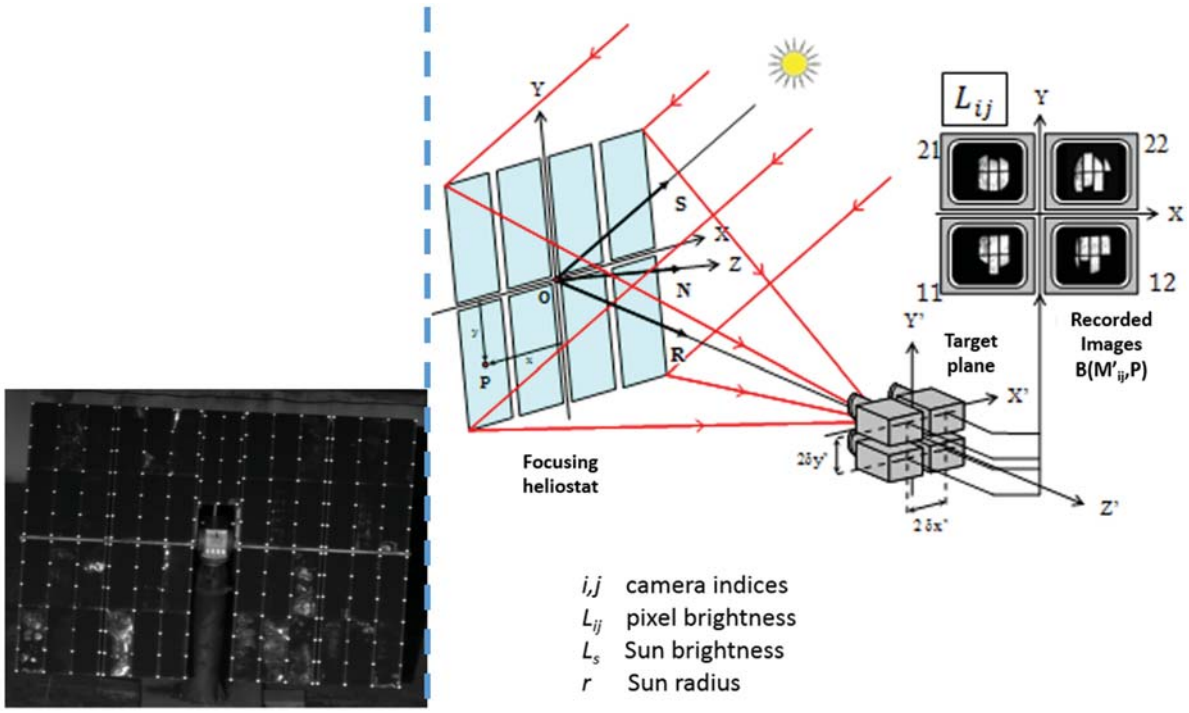

FIGURE 1. A heliostat of THEMIS used for experimentations (left) and the backward-gazing method principle (right).

BACKWARD-GAZING METHOD WITH FOUR CAMERAS

This method uses four cameras located in the target frame and simultaneously recording images of the Sun reflected by the optical surfaces. Combining the four images, data processing allows one to reconstruct the slopes and the shape errors of the surfaces. Image processing includes camera sensors and filters characteristics with geometrical transformations. Then, some numerical methods combine the four images to reconstruct the slopes of the mirrors [5].

The slope reconstruction was initially based on the Nijboer relations [4] linking the mirror slopes to the derivative of the wave front (method A) [6]. With this first version of the method A the effects of measurement noise were reduced by using an optimization algorithm but the effect of field rotation was not implemented in the process. To include the field rotation, new versions of this method (method A and O1) are presented in this article. These methods were more efficient than the early analytical slope reconstruction method presented in [4], but it can be improved for accuracy and decrease its sensitivity to measurement noise. The methods A and O1 needed slopes subtraction operations and angle calculations which increased the error sources. A new method is proposed in this article (method O2) which makes use of an a priori knowledge of the reflecting surface shape and reverse ray-tracing from the camera to the Sun. The reverse ray-tracing allows one to reconstruct the slopes more accurately and simplifies the computation by avoiding the geometrical transformations required to link the wave front slopes to the mirror slopes. Indeed, all referential changes are included in the ray-tracing algorithm.

NUMERICAL MODEL

Simulation of Experimentation with COSAC

COSAC (Simplified Optical Calculations for Combination Analysis) is a program in FORTRAN 77 developed by François Hénault [7] as part of a work on concentrated solar energy and optical space instruments. It is a ray-tracing program which allows to simulate hexagonal facets or focusing heliostat of a solar power plant. Reflection and refraction of rays are calculated for each optical surface, which are defined by an instruction file read by the program. Its performances are equivalent to the existing professional software. COSAC was chosen because of the

simplicity of outputting the brightness maps which are used to compute the slopes and for the freedom and opportunity to access the source code to modify it as needed. However, COSAC does not have the same graphic representation as ZEMAX or CODE V. The results of heliostat simulation are accessible in output files, including one that summarizes the results of the process and others that can be the brightness maps of the simulated heliostat or some other data ordered in the instruction file. In this study, a heliostat of the THEMIS tower power plant at Targassonne was simulated. The heliostat surface is more than 50 square meters and the four cameras are in a tower, close to the receiver at about a slant range of 120 meters from the heliostat. For the numerical validation of the reconstruction method, a heliostat was simulated with known defects on two of its modules. Each module is orientable by using three screws and defects can be entered by turning it. The nature of the entered defects in the simulations is supposed to be the same as that of the real entered defects on the heliostat of THEMIS, although their values are not exactly equal. It is supposed that the entered defects on the real heliostat are just canting errors and any mirror deformation is neglected. The defects are canting error of -1mrad and +1mrad around Y axis (elevation) on the 2nd and 3rd modules respectively. No azimuth defects are entered around X axis. We used two different Sun profile to generate the source and we compared the results. The first Sun profile is a modified version of the José formula [8] and the second one is a noisy Sun profile from a median calculation of actual Sun images. The heliostat, which is considered in Sun-tracking mode, reflects the Sun rays towards the four cameras. Therefore, the image of the Sun is observed through the heliostat, as in experimentation [Fig. 2].

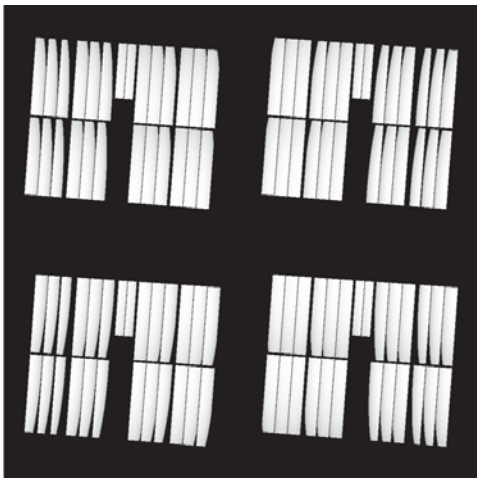

FIGURE 2. Four simulated images of a heliostat in sun-tracking mode generated by COSAC

Slopes Reconstruction with the Analytical Method (A)

The method A, which is presented in [4], is an analytical method based on the Nijboer relations. It links the mirror's slopes to the derivative of the wave front, itself linked to the brightness measured by the cameras. A function, which allows to find the angles of the incident rays from the measured brightness, is calculated. These angles are used to find the slopes of the wave front in the heliostat reference frame [4]. To compute the slopes, the images are post-processed with geometrical transformations that will permit image addition and subtractions. A mask was applied to eliminate the pixels with weak or no signal. The images are rotated and centred by using Fourier transformations and cross-correlations, respectively. Then we apply a transformation to have the same geometrical shape for every heliostats of the images. Henceforth, we can calculate the slopes by using the analytical method and get the derivative of the wave front along X and Y axis for each pixel. After calculating these slopes, we need to recalculate the cameras' coordinates, which are not the expected ones when the target vector of the heliostat is not perpendicular to the target plane, which is the most common case. Then we subtract the inherent aberrations of the heliostat to the slopes and we make some transformation, like the field rotation and the referential changings, to have the final ones, in the referential of the heliostat. The final results are two maps of the calculated slopes -which are the derivative of the heliostat's shape-, one along X axis and the other along Y axis.

Slopes Reconstruction with the First Optimisation Method (O1)

The method O1 is the first process used to overcome the weakness of the method A with noise measurement. The raw images need the same transformations as the previous method, but the analytical calculation of slopes is replaced by the use of a merit function. Instead of calculating analytically two slopes along X and Y axis for each pixel of the map, we vary the values of a couple of solutions and find the best one for each pixel. Each couple of solutions corresponds to a brightness value, which is compared to the value of the pixel by using the quadratic error. This process is done for all the cameras and the quadratic errors are added. The sum of the quadratic errors for all the cameras is the merit function. The couple of solutions, which minimizes the merit function, is then the best solution. An optimisation algorithm, based on Nelder-Mead algorithm [9], allows to converge to the best solution faster than with a simple test loop. Furthermore, the efficiency of this code is better when it starts directly with first-guess solutions. Therefore, we use the analytical results of the Method A as first-guess solutions. The results, which are the wave front's slopes as in the previous method, are treated in the same way to evaluate the derivative of the heliostat's shape.

Slopes Reconstruction with the Optimisation Method with Reverse Ray-Tracing (O2)

The method O2 [Fig. 4] is an improvement of the method O1, using a reverse ray-tracing process. The slopes are still calculated by using a merit function but the heliostat geometry is taken into account for each couple of solutions tested in the process. For each of these couples, the inverse path of a ray is traced from each cameras to the Sun and the corresponding brightness are compared to the value of the pixel by using the quadratic error, as the previous method. In this process, the shape of the heliostat and the referential changings are already taken into account for each traced ray. For the simulations, the shape of the heliostat is approximated by a sphere and the coordinates vector $\boldsymbol{OP}$ on the heliostat surface are calculated in the heliostat reference frame ($\boldsymbol{R_H}$) by taking into account its focal length $\boldsymbol{D}$ [Eq. 1] [Fig. 3]. The unitary vector $\boldsymbol{N_P}$ which is normal to the heliostat surface at point $\boldsymbol{P}$ is then calculated [Eq. 2] and these two vectors are expressed in the tower reference frame ($\boldsymbol{R_F}$) by using the azimuthal $\boldsymbol{a_N}$ and elevation $\boldsymbol{h_N}$ angles of the heliostat.

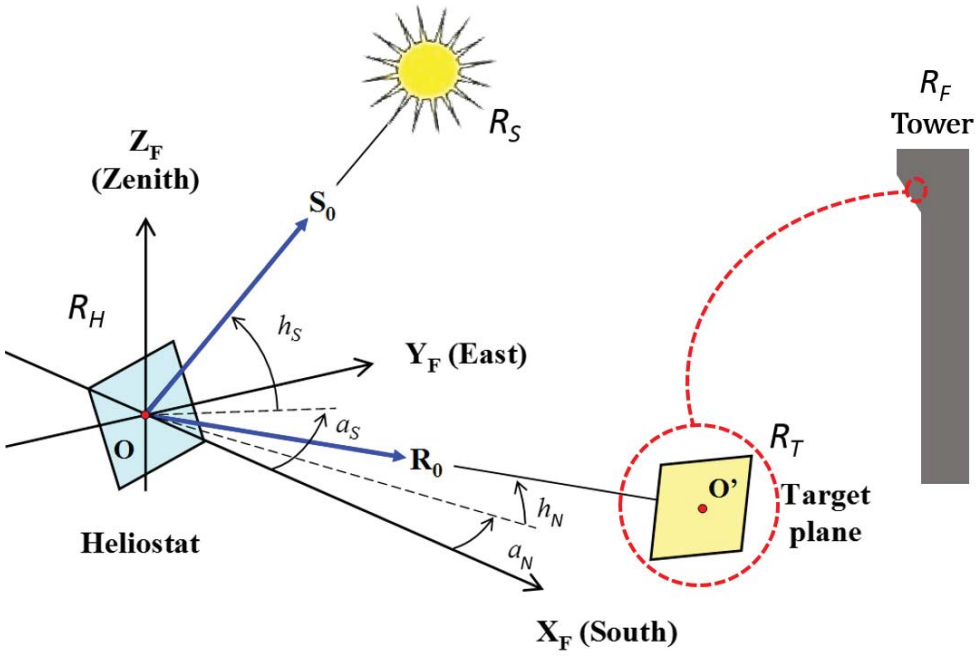

FIGURE 3. Simplified diagram of the different element of the experimentations on which are based the simulations.

$$\mathbf{OP}_{(R_H)} = \begin{pmatrix} x \\ y \\ z \end{pmatrix} = \begin{pmatrix} r^2/4D + r^4/64D^3 \\ y \\ z \end{pmatrix} \tag{1}$$

$$\mathbf{N}_{\mathbf{P}\,(R_H)} = \begin{pmatrix} u_{P\,(R_H)} \\ v_{P\,(R_H)} \\ w_{P\,(R_H)} \end{pmatrix} = \frac{1}{d'_P} \begin{pmatrix} 1 \\ \partial x(y,z)/\partial y - y\left(1 + r^2/8D^2\right)/2D \\ \partial x(y,z)/\partial z - z\left(1 + r^2/8D^2\right)/2D \end{pmatrix} \tag{2}$$

where $d'_P = \sqrt{1 + \left(\partial x(y,z)/\partial y - y\left(1 + r^2/8D^2\right)/2D\right)^2 + \left(\partial x(y,z)/\partial z - z\left(1 + r^2/8D^2\right)/2D\right)^2}$

The coordinates of the four cameras $\boldsymbol{M_i}$ are first expressed in the target reference frame ($\boldsymbol{R_T}$), which is inclined of 30 degrees compared to the vertical and then in the tower frame to calculate the direction of the reflected vectors from the heliostat [Eq. 3].

$$\mathbf{O'M''_i}_{(R_F)} = P_{(R'')\to(R_F)}\mathbf{O'M''_i}_{(R'')} = \begin{pmatrix} x_i \\ y_i \\ z_i \end{pmatrix} = \begin{bmatrix} \cos\pi/6 & 0 & -\sin\pi/6 \\ 0 & 1 & 0 \\ \sin\pi/6 & 0 & \cos\pi/6 \end{bmatrix} \begin{pmatrix} x''_i \\ y''_i \\ z''_i \end{pmatrix} \tag{3}$$

The vector $\boldsymbol{PM''_i}$, which correspond to the reflected ray from the heliostat toward the cameras, is then calculated by using [Eq. 1] and [Eq. 3], and its corresponding unitary vector is noted $\boldsymbol{R_{Pi}}$. By using the normal vector of the heliostat surface $\boldsymbol{N_{P\,(RF)}}$ and of the reflected rays $\boldsymbol{R_{Pi}}$, the vectors $\boldsymbol{S_{Pi\,(RF)}}$ from the heliostat to the Sun can be calculated by using the reflexion law of Descartes [Eq. 4]. They are expressed into the Sun reference frame ($\boldsymbol{R_S}$), by using the azimuthal $\boldsymbol{a_S}$ and elevation $\boldsymbol{h_S}$ angles of the Sun [Eq. 5]. The 2nd and 3rd components of $\boldsymbol{S_{Pi\,(RS)}}$ are used to find the angles $\boldsymbol{\varepsilon_i}$ [Eq. 6] and therefore to have the brightness.

$$\mathbf{S}_{\boldsymbol{Pi}\,(R_F)} = 2\left(\mathbf{N}_{\mathbf{P}\,(R_F)}\mathbf{R}_{\boldsymbol{Pi}\,(R_F)}\right)\mathbf{N}_{\mathbf{P}\,(R_F)} - \mathbf{R}_{\boldsymbol{Pi}\,(R_F)} \tag{4}$$

$$\mathbf{S}_{\boldsymbol{Pi}\,(\mathrm{R}_S)} = \begin{pmatrix} u_{Pi\,(R_S)} \\ v_{Pi\,(R_S)} \\ w_{Pi\,(R_S)} \end{pmatrix} = P_{(\mathrm{R}_F)\to(R_S)}\mathbf{S}_{\boldsymbol{Pi}\,(\mathrm{R}_F)} = \begin{bmatrix} \cos a_S \cos h_S & \sin a_S \cos h_S & \sin h_S \\ -\sin a_S & \cos a_S & 0 \\ -\cos a_S \sin h_S & -\sin a_S \sin h_S & \cos h_S \end{bmatrix} \begin{pmatrix} u_{Pi\,(R_F)} \\ v_{Pi\,(R_F)} \\ w_{Pi\,(R_F)} \end{pmatrix} \tag{5}$$

$$\varepsilon_i = \sqrt{v^2_{Pi\,(R_S)} + w^2_{Pi\,(R_S)}} \tag{6}$$

The optimization code converges to the lower value of merit function and uses the first-guess solutions of method A, as in the method O1. However, the results are directly in the final referential and the influence of the heliostat's shape is computed, so we don't need to apply the referential transformations and subtraction of heliostat inherent aberrations after the slopes calculations. All these advantages make it a more direct and faster method than the method O1.

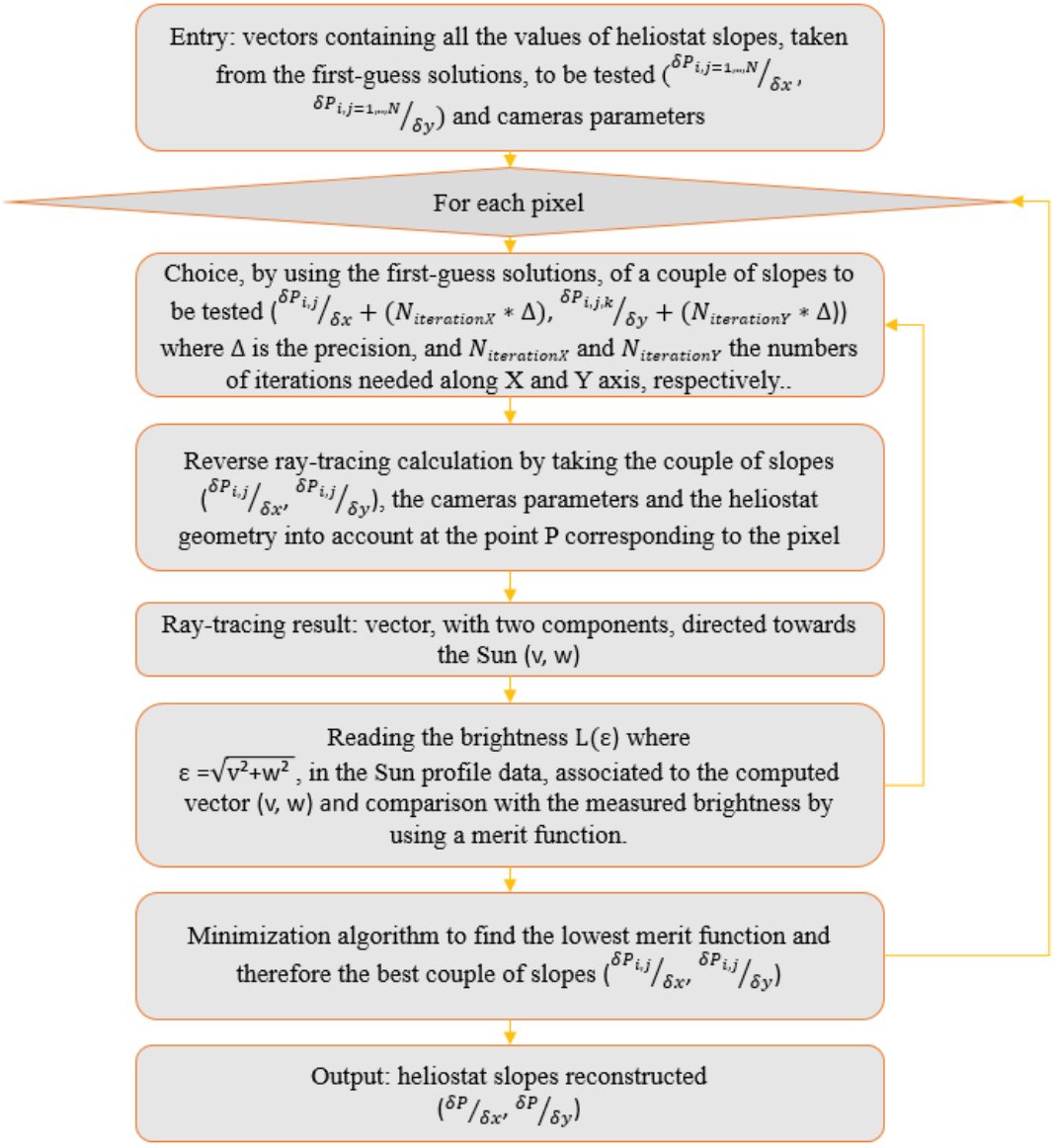

FIGURE 4. Simplified diagram of the method O2 process.

RESULTS AND DISCUSSION

The Measured and Analytical Sun Profiles Used for the Simulations

To simulate the reflection of a heliostat of a concentrated solar power plant, we need to generate a source which will act as the Sun. The Sun profile was already measured and its global appearance is relatively known, but it depends on the weather conditions of the experiment. In this context and for the experimentations and studies, the Sun's profile was measured, averaged (Fig. 5) and then used as input in COSAC software. The Sun profile contains points, each corresponding to a solar angle and a brightness value, and a threshold is applied to remove the signal on the circumsolar which is weaker than the noise measurement [Fig. 5].

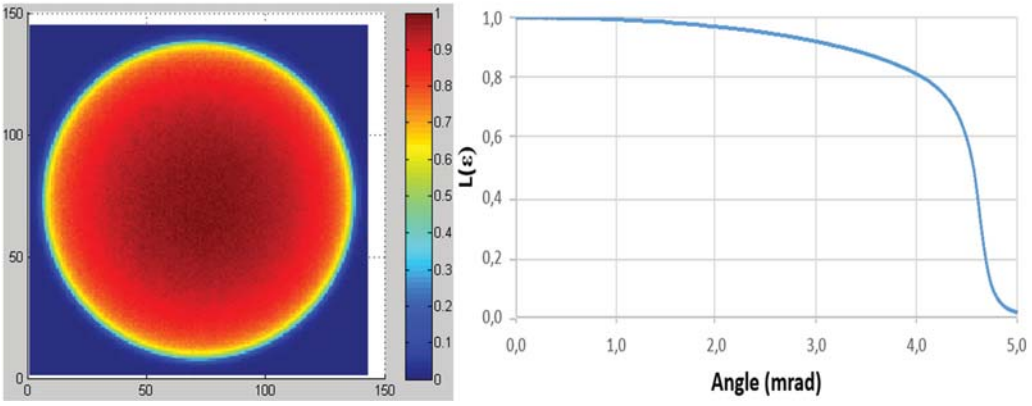

FIGURE 5. Median of 100 acquisitions of the Sun (left) and resultant measured profile (right).

The noisy Sun profile contains residual signal from the noise measurement of the camera and from the weather conditions. To test and validate the backward-gazing method by using simulations, a Sun profile without noise measurement is first needed [Fig. 6]. Therefore, a Sun profile based on the José formula was calculated [8] and the parameters were adjusted, which are the coefficient A and the power ξ –initially equal to 2-, to find the better similarity to the noisy Sun profile appearance as possible [Eq. 7]. The angles ε and ε_{MAX} express the apparent angle and the angular size of the Sun, respectively. This analytical profile is therefore used to validate the backward-gazing method and the measured one is used to test the robustness of the method with noise measurement.

$$A + (1 - A)\sqrt{1 - \left(\frac{\varepsilon}{\varepsilon_{MAX}}\right)^{\xi}} \tag{7}$$

where A = 0.679; ε_{MAX} = 4.360 and ξ = 2.222

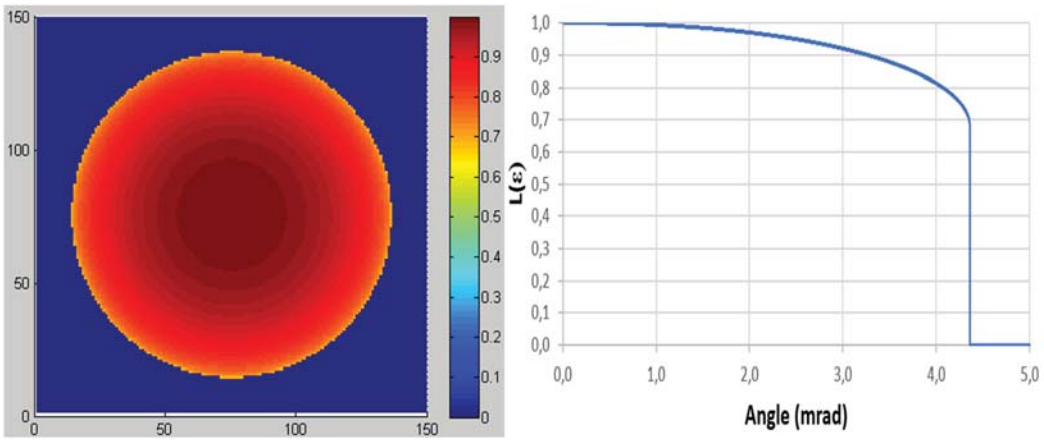

FIGURE 6. Sun from the modified formula of José (left) and its profile compared with the one from a noisy Sun until 4.360 milliradians (right).

Simulation of Slopes Reconstruction with the Analytical Method (A) with a Sun Profile from Modified Function of José and a Noisy Sun Profile

A heliostat was simulated without any defect with the Sun profile of modified formula of José as source. Then the heliostat was simulated with entered defects, which are -1mrad and +1mrad around X axis on the 2nd and 3rd module, respectively. The computing of the slopes for the two situations allows to subtract the slopes without defect to the slopes with defects, therefore isolate the slopes of the defects themselves [Fig. 7]. This method allows to show

if the data treatment is able to detect and quantify canting and curvature errors on the heliostat. The method A was first used for the data treatment. The relative slopes error is about 0.8% along the axis Y. But there is a contamination of data along the X axis for which the relative error is about 15%. Furthermore, the using of a noisy Sun profile as source, shows that the method A is too sensitive to noise. This time, the relative error is about 14.5% along X and more than 12% along Y axis. These results show that method A is not reliable enough when there is measurement noise, as in experimentation.

Simulation of Slopes Reconstruction with the First Optimization Method (O1) and a Sun Profile from Modified Function of José

By using an analytical Sun profile and entering the same defects as previously to the simulated heliostat, the relative slopes error is more than 14% along X axis and about 2% along Y axis. The contamination of the data along X axis is therefore less. When a noisy Sun profile is used, the results show that the method O1 is better to find the defect with a relative error about 8.6% along Y, but less accurate for the X axis with about 17% of relative error. These results show that the optimization code is better to find the slopes with the presence of noise measurement but that the contamination on the X axis is still high. This contamination is due to the uncertainty of the referential changes and of the subtraction of the heliostat inherent aberrations, which is done after the slopes' reconstruction. The calculation duration is longer than for the method A. These findings show that the optimization algorithm is improvable to become less sensitive to noise and data contamination.

Simulation of Slopes Reconstruction with the Optimization Method with Reverse Ray-Tracing (O2) and a Sun Profile from Modified Function of José

The results from the method O2 show that it is much better than the previous methods because more accurate and no sensitive to contamination of data along X axis [Fig. 8]. Furthermore, the reflections of the discarded facets contain the reflected areas of the Sun, which are closer to the circumsolar. These reflected areas can be a source of error because of their higher brightness's variation, therefore we applied an erosion process to remove the pixel's value near the edges of the reconstructed slopes and thus the aberrant slopes values. By using the analytical Sun profile, the relative error is about 0.5% along X and Y axis. With the noisy Sun profile, the relative error is about 1.3% along X and 2.9% along Y axis.

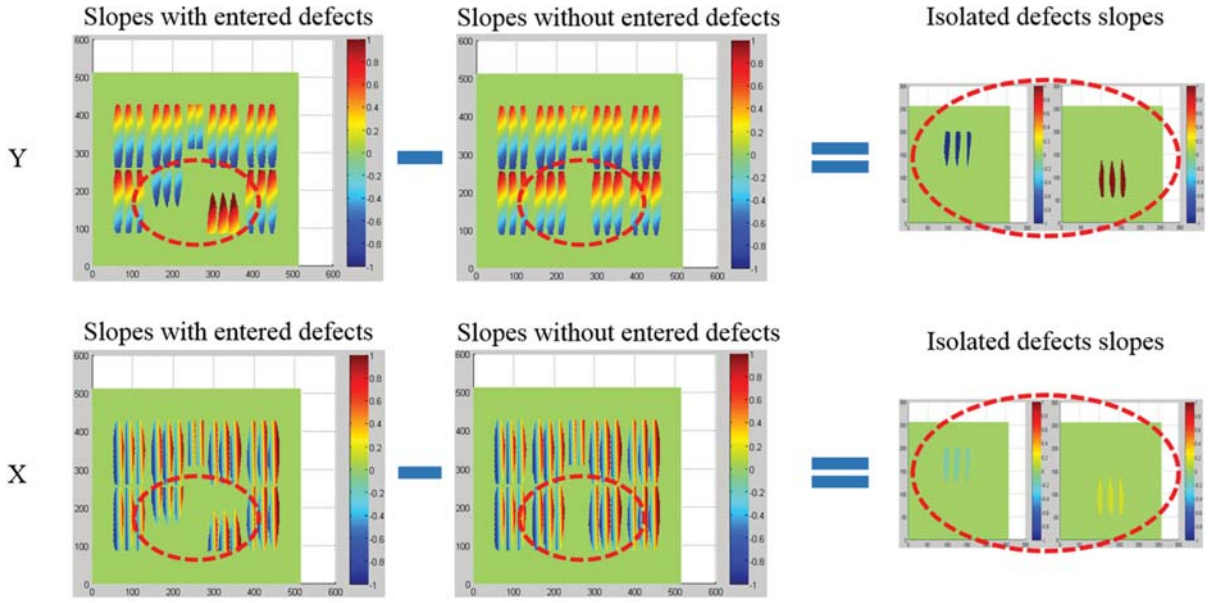

FIGURE 7. Slopes reconstructed with the method A and their subtraction to isolate the slopes of the entered defects.

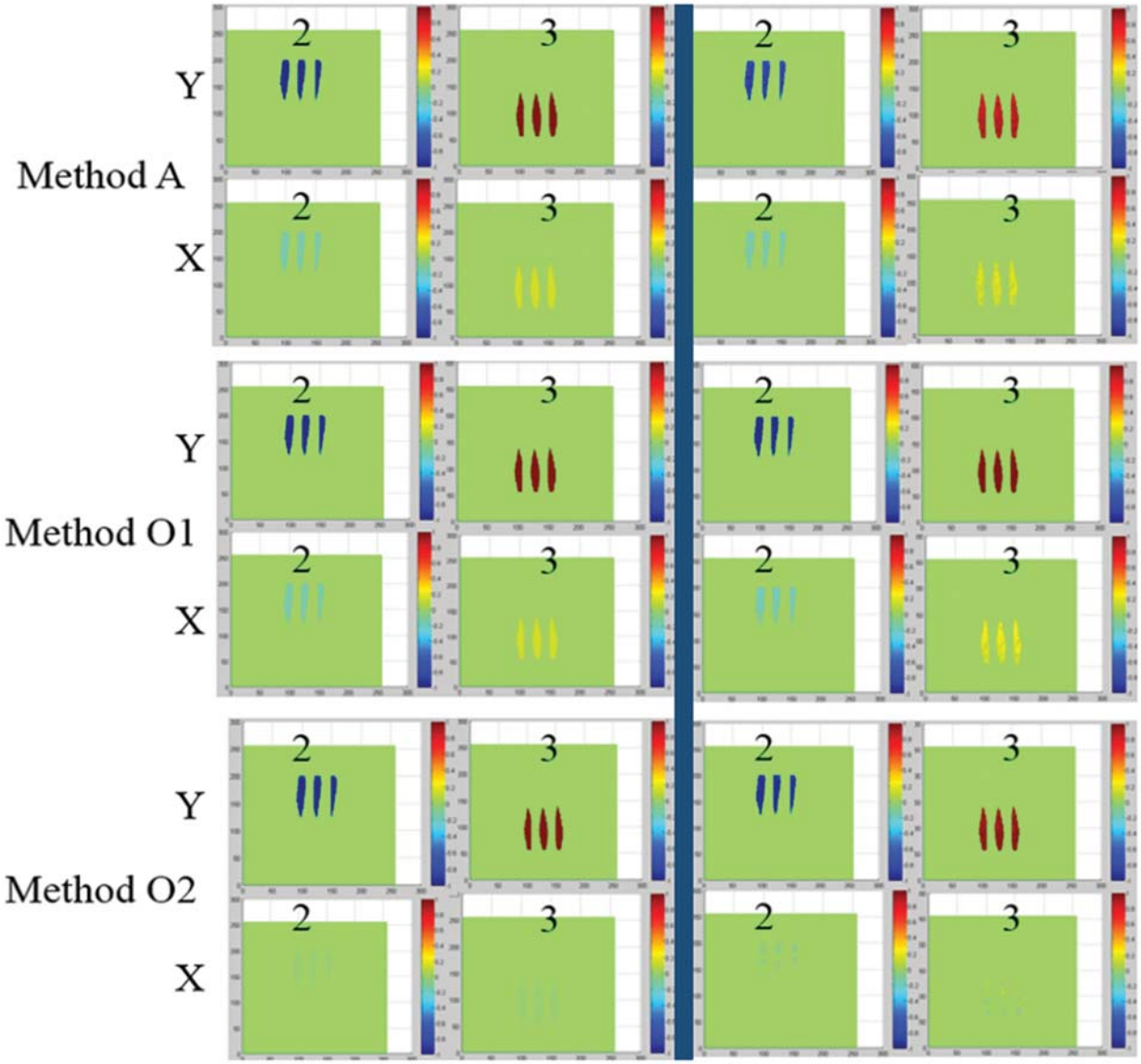

FIGURE 8. Slopes, on the modules n°2 and 3, of the simulated heliostat reconstructed by the three methods and by using an analytical Sun profile (left side); using a noisy Sun profile (right side).

Summary of the Different Methods

The three methods were tested by using a heliostat simulated with COSAC and by changing the quality of the source. The test with the method A showed the limitations of the use of an analytical calculation for the slopes' reconstruction. Moreover, the contamination of the slopes along X axis is the sign of a lack of precision of the referential changes, or of the subtraction of the heliostat inherent aberrations. When a noisy Sun profile is used the accuracy is worse along Y axis but steady along X axis. It shows that the analytical reconstruction is sensitive to noise. The method O1 takes the change of cameras' coordinates into account and uses an optimization algorithm for the slope reconstruction which is more efficient than the analytical one. We can see that the results along Y axis are better than the results of the method A when a noisy Sun profile is used, but there is still a contamination by false values of slopes along X axis. These results prove that the optimized reconstruction is less sensitive to noise, but the contamination along X axis shows that the referential changes are not precise enough. The method O2 is much more accurate than the previous methods along X and Y axis, even for an analytical Sun profile. There is no

contamination along X axis and the drop in precision of results, which occurs when a noisy Sun profile is used, is much less than with other methods. These results show that the use of reverse ray-tracing in the optimization algorithm is better to take the referential changes and the inherent aberrations of the heliostat into account. The reached accuracy -less than 1% for an analytical Sun profile and less than 4.5% for a measured one- is higher than the objective of the backward-gazing method which is 10% of 1 mrad.

TABLE 1. Summary of the relative errors of reconstructed slopes for the three methods.

Method	Sun Profile	Module	
		2	3
		Relative Error Compared to 1 mrad along X / Y Axis (%)	
Analytical (A)	Generalized José Formula	15.5 / 0.7	14.7 / 0.9
	Measured with Noise	14.6 / 11.6	14.2 / 13.1
Optimized (O1)	Generalized José Formula	14.7 / 1.8	13.8 / 2.1
	Measured with Noise	16.3 / 10.1	17.8 / 7.1
Optimized with Reverse Ray-Tracing (O2)	Generalized José Formula	0.5 / 0.6	0.5 / 0.5
	Measured with Noise	1.5 / 1.6	1.1 / 4.2

CONCLUSION

The three methods were tested by using an ideal heliostat and by choosing the kind of source needed for their validation. This process is based on the simulation of a heliostat of the THEMIS power plant at Targassonne and it allows to generate some entered defects to its modules. Having simulated images allows to test the registration process of the backward-gazing method and the final subtraction of the reconstructions -with and without entered defects- allows to isolate these defects and quantify the relative error of each method. The methods A showed its limitation by the contamination of the slopes along X axis, which causes a relative error that is too high for the targeted accuracy, as its sensitivity to noise measurement, which is present in the images simulated with a noisy Sun profile. Due to its optimized reconstruction, the method O1 is better than the previous one when a noisy Sun profile is used, but there is still a high contamination along X axis. The reverse ray-tracing process of the method O2, coupled to its optimization code, allows to have more accurate results –with a relative error less than 4.5%- for analytical and noisy Sun profile. The reasons are a higher robustness to noise measurement and the suppression of the contamination along X axis, both due to the reverse ray-tracing which takes the heliostat geometry into account directly in the process. With the better performances of the method O2, the detection accuracy of waviness, mirror canting and heliostat pointing errors will be improved. The new reconstruction process will simplify future work on the use of a 2D Sun profile instead of a 1D profile. In this study, the nature of the Sun profile was changed but the heliostat is still an ideal one. However, the complete validation of the backward-gazing method will require the use of experimental images of heliostat to test the robustness of the method in real conditions.

FUNDING AND ACKNOWLEDGEMENTS

This project has received funding from the European Union's Horizon 2020 research and innovation programme under grant agreement No 727762, Next-CSP project and was supported by the French "Investments for the future" ("Investissements d'Avenir") programme managed by the National Agency for Research (ANR) under contracts ANR-10-LABX-22-01 (Labex SOLSTICE) and ANR-10-EQPX-49 (Equipex SOCRATE).

REFERENCES

1. Arancibia-Bulnes, C.A., Peña-Cruz, M.I., Mutuberría, A., Díaz-Uribe, R., Sánchez-González, M., (2017). A survey of methods for the evaluation of reflective solar concentrator optics. Renew. Sustain. Energy Rev. 69, 673–684.
2. F. Henault, C. Caliot, (2014), Facility for concentrating cosmic radiation equipped with a reflective optical surface control system, WO2015144699.

3. F. Henault, C. Royere. Concentration du rayonnement solaire : analyse et évaluation des défauts de réglage de facettes réfléchissantes. Revue de Physique Appliquée, 1989, 24 (5), pp.563-576.
4. Coquand, M., Hénault, F., Caliot, C., (2017a). Backward-gazing method for measuring solar concentrators shape errors. Appl. Opt. 56, 2029–2037.
5. Coquand, M., Caliot, C, Hénault, F., (2017). Tracking and shape errors measurement of concentrating heliostats. Proc. of SPIE vol. 10379 103790N-1.
6. Coquand, M., Hénault, F., Caliot, C., (2018). Numerical identification of mirror shapes with the backward-gazing method using an actual solar profile. AIP Conference Proceedings, SolarPACES 2017, 2033, 040010.
7. F. Hénault, COSAC version 2.9.7. Présentation générale, URL http://francois.henault.free.fr/cosac/download/cosac_doc1.pdf (2019).
8. P. Jose, "The flux through the focal spot of a solar furnace," Solar Energy vol. 1, p. 19-22 (1957).
9. Nelder, J.A. and Mead, R. (1965), "A simplex method for function minimization", Comput. J., 7, pp. 308–313.